

# Clustering in two models of interacting motors

**Jim Chacko<sup>1</sup> \*, Sudipto Muhuri<sup>2</sup> † and Goutam Tripathy<sup>3,4</sup> #**

<sup>1</sup> Christian College, Angadical South PO, Chengannur, Kerala 689122, India.

<sup>2</sup> Department of Physics, Savitribai Phule University of Pune, Pune Maharashtra 411 007, India.

<sup>3</sup> Institute Of Physics, Sachivalaya Marg, Sainik School PO, Bhubaneswar 751005, India.

<sup>4</sup> Homi Bhabha National Institute, Anushaktigar, Mumbai 400094, India.

E-mail: \* [jim.chacko.v@gmail.com](mailto:jim.chacko.v@gmail.com), † [muhuri@physics.unipune.ac.in](mailto:muhuri@physics.unipune.ac.in),

# [goutam@iopb.res.in](mailto:goutam@iopb.res.in)

**Abstract.** We study a two-species bidirectional exclusion process, and a single species variant, which is motivated by the motion of organelles and vesicles along microtubules. Specifically, we are interested in the clustering of the particles and appearance of a single large cluster as the ratio  $Q$  of the translation to switching rates is varied. We find that, although for a finite system, there is a clustering phenomenon in which the probability of finding a single large cluster changes from being negligible to having finite values, the phenomenon shifts to larger  $Q$  values as the system size is increased. This suggests that the observed clustering is not a true (non-equilibrium) transition in the thermodynamic sense but rather a finite-size effect.

## 1. Introduction

One-dimensional driven lattice gas models have been the subject of considerable interest due their remarkably rich stationary and dynamical behaviour [1]. Further, the inherent simplicity of these models are useful for application to diverse phenomena [2, 3] including those in biology [4].

Bidirectional transport of cargo vesicles and organelles along one-dimensional cytoskeletal filaments has been observed in context of intracellular transport and studied fairly extensively for the dynamics of pigment granules in melanophores [5], mitochondria in the axons of neuronal cells [6, 7], endosomes in *Dictyostelium* cells [8] and lipid-droplets in *Drosophila* embryos [9, 10]. Bidirectionality is achieved by the collective action of oppositely directed motor proteins (such as kinesin and dynein) which results in the translation of the cargo along the filament along with the directional switching of the transported cellular cargo [11, 12].

The interplay of the switching dynamics of individual particles and the collective movement of particles in 1D has been studied theoretically using a two species lattice gas model in [13]. There, it has been shown that if the directional switching rate ( $\alpha$ ) is much faster than the translation rate ( $v$ ), the steady state density and current profiles of the particles are homogeneous in the bulk and are well described by a mean field theory, and the model could be mapped to the exactly solvable Partially Asymmetric Exclusion Process (PASEP) [14]. Furthermore, it has been argued that the mean field theory fails away from this fast switching limit, and the steady state behaviour is characterized as a function of the ratio  $Q = v/\alpha$  of the translation and net switching rates. In [13], it was observed that in the limit of very slow switching rates (compared to the translation rates), the system approaches a jammed phase with a net current that tends to zero as  $J \sim 1/Q$ . It was further argued that in many realistic cellular situations involving transport of cellular cargo, such as transport of lipid-droplets in wild type *Drosophila* embryos [10], the switching rates are much slower than the translation rates so that  $Q$  is high. This would, in turn, imply an enhanced tendency of jamming of these cargo aggregates and formation of clusters during the transport on the cellular filament. This naturally invites the question as to how  $Q$  affects the cluster size distribution of these cellular cargoes involved in bidirectional transport. We study this issue within the framework of a minimal model which is defined on a one-dimensional lattice and described in Ref.[13]. However, unlike as in [13], where lattice with open boundary is considered, we study this model by imposing periodic boundary condition on the lattice and thereby also fixing the density of vacancies on the lattice.

We first study the cluster size distribution of particles for the minimal model using Monte Carlo simulations for a wide range of  $Q$ . We look at the cluster size distribution in the steady state and see the appearance a single large cluster (the aggregate) as the value of  $Q$  is increased value. We study the probability of occurrence of this large cluster for different system sizes  $L$  as well as the density  $\rho$  of particles. Although, the appearance of a large aggregate seems like a nonequilibrium phase transition, we find

that, for a given  $Q$ , as the system size is increased the probability of the large cluster decreases and eventually it disappears. We further study another model derived by tweaking the minimal model in which similar chipping and aggregation mechanisms of particles exist but with a single species of particles. While it shares qualitative features of the minimal model, there are quantitative differences.

## 2. Two Species Bidirectional Exclusion Process

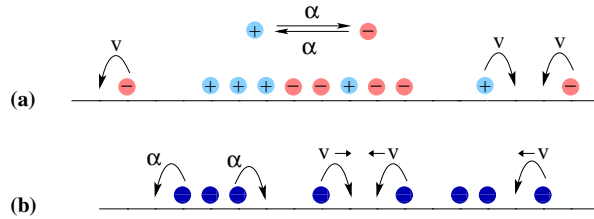


**Figure 1.** Schematic representation of the dynamical processes for (a) the Two Species Bidirectional Exclusion Process (2S-BEP). (b) the Symmetric Exclusion Process with Directional Memory (SEP-DM).

We mimic the microtubule - molecular motor - vesicle system as a Two Species Bidirectional Exclusion Process (2S-BEP) in the following manner. We represent a single microtubule filament as a one-dimensional lattice with  $L$  sites (Fig. 1(a)). The cellular cargo carried by the collective action of motors, is considered here as a particle; it can either be in the  $\oplus$  state (moving anticlockwise) or in the  $\ominus$  state (moving clockwise), with a fixed rate of switching  $\alpha$  between the two states [15]. The switching may be thought of as a result of a tug-of-war mechanism by oppositely directed motors or by external regulation [7]. The two states of the particles can, in turn, be regarded as particles of two species. Each lattice site  $i$  is either vacant or occupied by a particle - either  $\oplus$  or  $\ominus$ . The  $\oplus$  and  $\ominus$  translocate to the adjacent vacant site on the right or left respectively with a rate  $v$ . In all our simulations, initially, equal number of particles of both species are taken. The various dynamical processes are schematically displayed in Fig. 1(a). The total density of particles (of both types together) is denoted by  $\rho$  and is conserved under the dynamics, but number/density of each type of particles is not conserved separately.

We study the 2S-BEP using Monte Carlo simulations. For a given system size  $L$  and overall particle density  $\rho$ , the initial condition is a random distribution of  $N = L\rho$  particles over  $L$  sites. In one microstep, a site is chosen randomly, and if it is occupied its sign is changed with rate  $\alpha$  and is moved to its appropriate (empty) neighbouring site with rate  $v$ .  $L$  such microsteps constitute one MC step. We evolve the system for  $T_0$  MC steps to reach steady state and compute various steady state averages over further  $T$  MC steps. We further, do an ensemble average over  $M$  realizations of initial conditions. Range of values of these quantities in our simulations are:  $T_0 \sim 10^5 - 10^6$ ,

$T \sim 10^7 - 10^8$ , and  $M \sim 10^4 - 10^5$ .

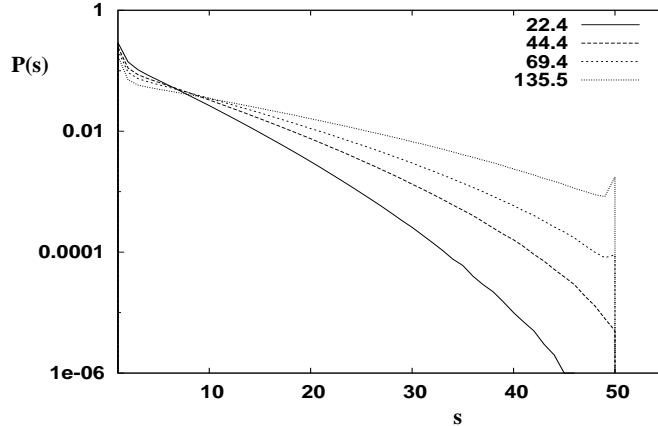


**Figure 2.** Cluster size distribution  $P(s)$  for  $L = 50$  and density  $\rho = 0.5$  for different values of  $Q$ .

Particles of each species undergo a totally asymmetric exclusion dynamics in opposite directions depending on its sign. A cluster consists of a group of particles of any sign bounded by two vacant sites and no holes in between (no distinction is made between the kinds of particles while determining the size of a cluster). The smallest blockage is formed if a  $\dots \oplus \ominus \dots$  configuration occurs on the lattice - the only way for it to disappear is by a switching the type of either one of the particles. For small values of  $Q$   $O(1)$ , both types of particles move almost freely on the lattice. Although blockages do form occasionally, the clusters do not grow to large sizes.

As the value of  $Q$  is increased (in our simulations we fix the value of  $v$  and change  $\alpha$  to vary  $Q$ ), clusters of different sizes begin to form. We obtain the probability distribution  $P(s)$  of cluster sizes averaged over time  $T$  and number of realizations  $M$  of initial conditions. In Fig. 2, we plot the cluster size distribution  $P(s)$  vs  $s$  for a number of values of  $Q$  for  $L = 50$  and  $\rho = 0.5$ . We observe that as  $Q$  is increased,  $P(s)$  broadens and larger clusters begin to form [16]. We denote by  $P(s_{max})$  the probability of the largest cluster of particles (by definition the largest cluster has all the particles,  $s_{max} = \rho L$ ). From Fig. 2, it appears that beyond a critical value of  $Q$ ,  $P(s)$  becomes non-monotonic and a local peak appears in the  $P(s)$  plot at the largest cluster size  $s_{max}$ . This raises the question whether the appearance of the largest cluster is a (nonequilibrium) transition. Below we present evidence that this is not a transition in the usual thermodynamic sense.

In Fig. 3, we plot variation of  $P(s_{max})$  as a function of  $Q$  for a given density  $\rho = 0.5$  and for three system sizes  $L = 100, 200, 400$ . Although, for each system size it appears that the single large cluster occurs for  $Q$  beyond a critical value  $Q_c$ , i.e.,  $P(s_{max}) = 0$  for  $Q < Q_c$ . However, upon longer steady state averaging the value of  $Q_c$  appears to be lowered. More importantly, as the system size is increased, it is seen that, for a given  $Q$ , the value of  $P(s_{max})$  decreases. I.e., in the thermodynamic limit  $L \rightarrow \infty$ ,  $P(s_{max}) \rightarrow 0$ .

Thus, the phenomenon of formation of the single aggregate as a function of  $Q$  is not a true transition in the thermodynamic sense.

We also compute the variation of  $P(s_{max})$  as a function of  $Q$  for a given system size  $L = 100$  and for a number of densities  $\rho$  and the data is shown in Fig. 4. We notice a  $\rho \leftrightarrow (1 - \rho)$  symmetry of the plots. This is due to the fact that  $P(s_{max})$  is the same for the cluster size distribution of the particles  $P(s; \rho)$  and the vacant sites  $P(s_h; \rho)$  since the appearance of the largest aggregate for both are concomitant.

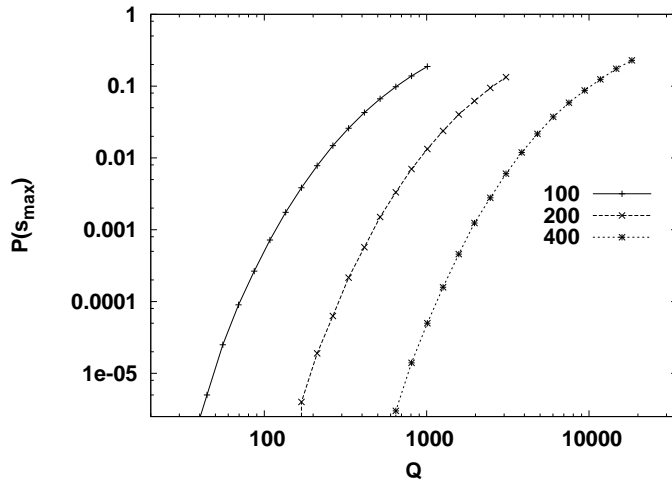


**Figure 3.**  $P(s_{max})$  vs  $Q$  for  $L = 100, 200$  and  $400$  and  $\rho = 0.5$  for the 2S-BEP.

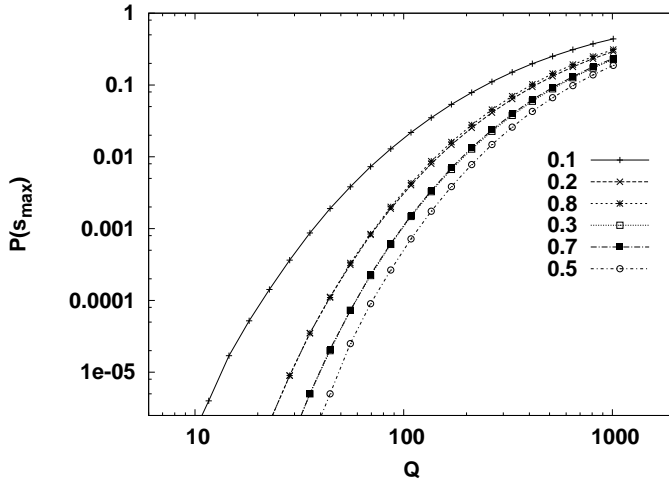


**Figure 4.**  $P(s_{max})$  vs  $Q$  for  $L = 100$  and total density of particles  $\rho = 0.1, 0.2, 0.3, 0.5, 0.7$  and  $0.8$  for the 2S-BEP. The  $\rho \leftrightarrow 1 - \rho$  symmetry is to be noted.

Although, the clustering seen for large  $Q$  is not a true critical transition, nevertheless, we notice an interesting scaling in the nature of  $P(s_{max})$  vs  $Q$  plots for

different  $L$  and  $\rho$  values as follows,

$$P(s_{max}) = F\left[\frac{Q}{L^\mu \rho(1-\rho)}\right]; \quad \mu = 2. \quad (1)$$

The data collapse via Eq. (1) of the data shown in Figs. 3, 4 is shown in Fig. 5.

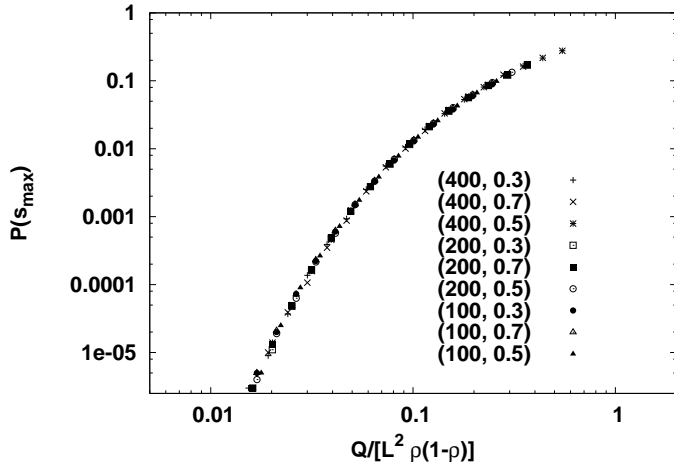


**Figure 5.** Data collapse of  $P(s_{max})$  vs  $Q/(L^2 \rho(1-\rho))$  for the 2S-BEP for  $L = 100, 200$  and  $400$  for  $\rho = 0.3, 0.5$  and  $0.7$ .

We also computed the mean cluster size for the particles and find that  $\langle s_p \rangle \sim \sqrt{Q}$  for smaller values of  $Q \ll L^2$  (Fig.6). The mean cluster size for the vacant sites  $\langle s_h \rangle \sim \sqrt{Q}$  as well. As  $Q$  increases, the mean particle and vacancy cluster size increase and saturate at  $L\rho$  and  $L(1-\rho)$  respectively, as  $Q \rightarrow \infty$ , corresponding to the single largest cluster. These observations can be combined in to a single scaling function for the mean cluster size as

$$\langle s_p \rangle = f(\rho) Q^\phi Y\left(\frac{Q}{g(\rho)L^{1/\phi}}\right); \quad Y(u \rightarrow 0) = 1, \quad Y(u \rightarrow \infty) = u^{-\phi}. \quad (2)$$

To ensure that the asymptotic  $\langle s_p \rangle = L\rho$ , we must have  $f(\rho)[g(\rho)]^\phi = \rho$ . The data of Fig. 6 is consistent with the value of the scaling exponent  $\phi = 1/2$ . We further conjecture that the two exponents  $\mu$  and  $\phi$  are indeed related as

$$\phi = \frac{1}{\mu}. \quad (3)$$

### 3. Symmetric Exclusion Process with Directional Memory

The 2S-BEP discussed in the previous section is a two-species model with particle moves specified by two rates,  $v$  and  $\alpha$ . It displays a clustering of particles when the ratio  $Q = v/\alpha$  is increased.  $P(s_{max})$ , the probability to find the largest cluster, has

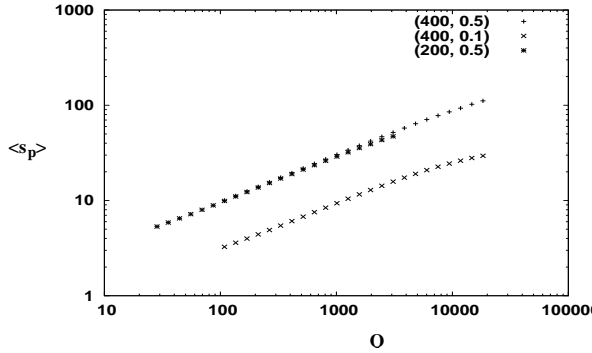


**Figure 6.** The mean cluster size of particles  $\langle s_p \rangle$  vs  $Q$  for  $(L, \rho) = (400, 0.5)$ ,  $(400, 0.1)$  and  $(200, 0.5)$  for the 2S-BEP.  $\langle s_p \rangle \sim \sqrt{Q}$  for the 2S-BEP.

a  $\rho \longleftrightarrow (1 - \rho)$  symmetry as well as a system size dependence. The clusters in the two-species model grow or fragment when a  $+$ ( $-$ ) species switches to a  $-$ ( $+$ ) and hops to the left (right) until it attaches to the right (left) of another cluster (or itself, in the case when only one large cluster exists). Retaining this feature, i.e., the directionality of motion of the particles that chips off from a cluster, we introduce a single species model, namely, the Symmetric Exclusion Process with a Directional Memory (SEP-DM).

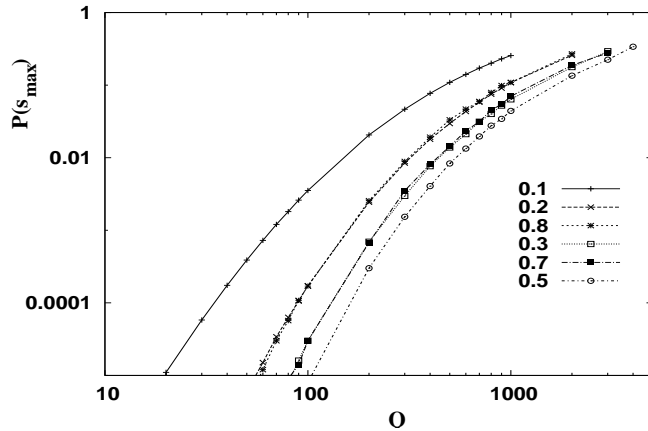


**Figure 7.**  $P(s_{max})$  vs  $Q$  for SEP-DM for a system of size  $L = 100$  and different density of particles  $\rho = 0.1, 0.2, 0.3, 0.5, 0.7$  and  $0.8$ . Note the  $\rho \leftrightarrow 1 - \rho$  symmetry.

The model is defined on a 1D lattice of  $L$  sites with periodic boundary conditions (Fig. 1b). The dynamics of the particles are as follows. A particle chips off from the left or right end of a cluster with a rate  $\alpha$  and keeps moving in the same direction (i.e. the particle breaking off from the left end will keep moving left/clockwise and one breaking off from the right edge will keep moving right/anti-clockwise) with a rate  $v$  until it attaches itself to the neighbouring cluster.

In the same spirit as in the case of 2S-BEP, we define  $Q = v/\alpha$  to be the ratio of rate of translocation (hopping of single free particle) to the rate of detachment of

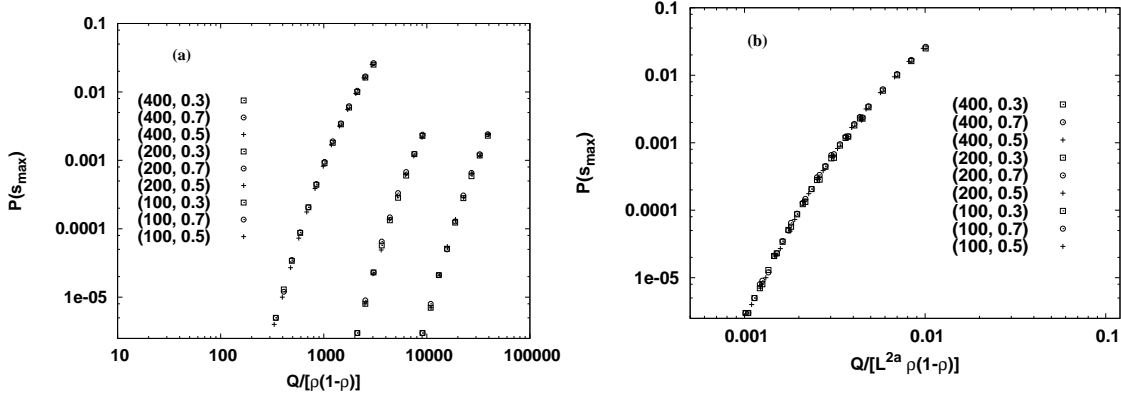


**Figure 8.** (a)  $P(s_{max})$  vs  $(Q/(\rho(1-\rho))$  for the SEP-DM for three system sizes:  $L = 100, 200, 400$  for the densities  $\rho = 0.3, 0.5$  and  $0.7$ . (b) The scaling collapse of  $P(s_{max})$  vs  $Q$  via Eq. (1) but with  $\mu = 8/3$ .

a particle from a cluster. We study the SEP-DM using Monte Carlo simulations. For a given system size  $L$  and overall particle density  $\rho$ , the initial condition is a random distribution of  $N = L\rho$  particles. We evolve the system for  $T_0$  MC steps to reach steady state and compute various steady state averages over further  $T$  MC steps. We further do an ensemble average over  $M$  realizations of initial conditions. Range of values of these quantities in our simulations are:  $T_0 \sim 10^5 - 10^6$ ,  $T \sim 10^7 - 10^8$  and  $M \sim 10^4 - 10^5$ .

Due to the directional memory feature mimicking the movements of two species of particles in the 2S-BEP, we expect the SEP-DM to have, at least qualitatively, similar behaviour as the 2S-BEP. We plot the probability of the largest cluster  $P(s_{max})$  as a function of  $Q$  for a number of densities  $\rho$  for a system size  $L = 100$  in Fig. 7. The data shows the  $\rho \leftrightarrow (1-\rho)$  symmetry also seen in the 2S-BEP model. In Fig. 8(a), we plot  $P(s_{max})$  vs  $\frac{Q}{\rho(1-\rho)}$ , taking in to account this symmetry, for three different system sizes  $L$ . It is seen from this plot that as  $L$  increases  $P(s_{max})$  decreases for the same value of  $Q$ . This implies that the appearance of the single cluster is not a true transition in the case of the SEP-DM as well, as may be expected.

It turns out that a scaling collapse of the  $P(s_{max})$  vs  $Q$  data for different  $L$  and  $\rho$ , values is possible with the scaling form given in Eq. (1) but with  $\mu = 8/3$ . This is shown in Fig. 8(b).

We also computed the mean cluster size of particles for SEP-DM as a function of  $Q$  and find that the data is consistent with  $\langle s_p \rangle \sim Q^{3/8}$  for smaller values of  $Q$  (Fig.6). As  $Q$  increases, the mean cluster size increases and saturate at  $L\rho$ , as  $Q \rightarrow \infty$ , corresponding to the single largest cluster. Thus, the  $L$  and  $\rho$  dependence of the mean cluster size can be put in the scaling form of Eq. (2) with  $\phi = 3/8$ . It is interesting to note that the relationship Eq.(3) between the two exponents  $\mu$  and  $\phi$  holds in this case as well.

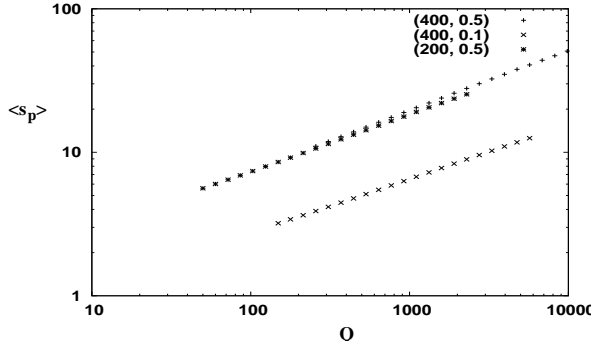


**Figure 9.** The mean cluster size of particles  $\langle s_p \rangle$  vs  $Q$  for  $(L, \rho) = (400, 0.5)$ ,  $(400, 0.1)$  and  $(200, 0.5)$  for the SEP-DM. The slope of the plots for smaller  $Q$ 's is consistent with a value of  $3/8$ .

#### 4. Conclusion

In this paper, we have studied a two-species bidirectional exclusion process which was motivated by the motion of organelles and vesicles along microtubules. Specifically, we were interested in the clustering of the particles and appearance of a single large cluster as the ratio  $Q$  of the translation to switching rates is varied. We found that although for a finite system, there appears to be a clustering phenomena in which the probability of finding the single large cluster changes from being negligible to having appreciable finite values, the phenomena shifts to larger  $Q$  values as the system size was increased. This suggests that the observed transition is not a true transition in the thermodynamic sense but rather a finite-size effect.

We further studied a single species version of the above model in which the directional memory of the detached particle is incorporated. This model also shows qualitatively similar clustering phenomena which vanishes in the thermodynamic limit.

In both models, the probability of occurrence of the largest cluster and mean cluster size as functions of  $Q$  shows nontrivial dependence on system size  $L$  and overall density  $\rho$  which can be characterized by scaling functions with corresponding exponents. Analytical understanding of these scaling forms and the values of the scaling exponents remain open for further investigations.

We would like to comment on a few other one dimensional (1D) models where such apparent transitions as well as finite-size effects have been reported. Consider the symmetric conserved mass aggregation model where a mass may diffuse as a whole or a part of it may chip off [17]. In this model, the distribution of mass at each site undergoes a transition from an exponential to a power-law as the overall density is increased. Beyond this critical density, the power-law distribution is unchanged; the extra mass appears as an infinite aggregate - a single large mass which is a finite fraction of the total mass in the system. If the jumps to the left and right are made asymmetric, this transition is not possible [18]. Although, in simulations, the transition as well as the

infinite aggregate is observed - this was attributed to finite-size effects.

Further, if the rate of diffusion of the mass as a whole were not constant, as in the above, but mass dependent ( $\sim m^{-\gamma}$  with  $\gamma > 0$ ) [18], although the simulations show a transition from the exponential mass distribution to a power-law with an infinite aggregate as the density was increased, it turns out that here too, this is only a finite-size effect and the model does not show a true transition.

Another example of an apparent phase transition reported in [19], the finite-size effects are discussed in [20].

## References

- [1] G. M. Schütz, J. Phys. A: Math. Gen. **36** R339 (2003).
- [2] D. Helbing, Rev. Mod. Phys. **73** 1067 (2001).
- [3] L. P. Kadanoff, Rev. Mod. Phys. **71**, 435 (1999).
- [4] T. Chou and D. Lohse, Phys. Rev. Lett. **82** 3552 (1999).
- [5] V. I. Rodionov, A. G. Hope, T. M. Svitkina and G. G. Borisy, Curr. Biol. **8**, 165 (1998).
- [6] R. L. Morris and P. J. Hollenbeck, J. Cell. Sc. **104**, 917 (1993).
- [7] M. A. Welte, Curr. Biol. **14**, R525 (2004).
- [8] V. Soppina, A.K. Rai, A. J. Ramaiya, P. Barak and R. Mallik, Proc. Nat. Acad. Sci. **106**, 19381 (2009).
- [9] M. J. I. Müller, S. Klumpp and R. Lipowsky, Proc. Nat. Acad. Sci. **105**, 4609 (2008).
- [10] S.P. Gross, M. A. Welte and E. F. Wieschaus, J. Cell. Biol **156**, 715 (2002).
- [11] B. Alberts et al., *Molecular Biology of the Cell* ( Garland Science, New York, 2002).
- [12] J. Howard, *Mechanics of Motor Proteins and the Cytoskeleton*, (Sinauer Associates, Massachusetts, 2001).
- [13] S. Muhuri, L. Shagolsem and M. Rao, Phys. Rev. E. **84** 031921 (2011).
- [14] S. Sandow, Phys. Rev. E. **50**, 2660 (1994).
- [15] For unequal rate of switching,  $\alpha_+(\alpha_-)$  being the rate of interconversion from a right (left) moving state to a left (right) moving state, we observe that the cluster only tends to drift along the lattice towards the left (right) for  $\alpha_+ < \alpha_-$  ( $\alpha_+ > \alpha_-$ ). In this work, we have taken them to be equal as our interest is in the cluster-size distributions and the jammed state.
- [16] As  $Q$  is increased from 1, the distribution of size of the clusters seems to change from an exponential to a stretched-exponential.
- [17] S. N. Majumdar, S. Krishnamurthy, and M. Barma, Phys. Rev. Lett. **81**, 3691 (1998); J. Stat. Phys **99**, 1 (2000).

- [18] R. Rajesh and S. Krishnamurthy, Phys. Rev. E **66**, 046132 (2002); R. Rajesh, D. Das, B. Chakraborty, and M. Barma, Phys. Rev. E **66**, 056104 (2002).
- [19] P.F. Arndt, T. Heinzel, and V. Rittenberg, J. Phys. A **31**, L45 (1998), J. Stat. Phys. **97**, 1 (1999); N. Rajewsky, T. Sasamoto, and E.R. Speer, Physica A **279**, 123 (2000); T. Sasamoto and D. Zagier, J. Phys. A **34**, 5033 (2001).
- [20] Y. Kafri, E. Levine, D. Mukamel, G. M. Schütz, and J. Török, Phys. Rev. Lett. **89**, 035702 (2002); Y. Kafri, E. Levine, D. Mukamel, G. M. Schütz, and R. D. Willmann, Phys. Rev. E **68**, 035101 (2003).